arXiv:1405.7824v1 [physics.flu-dyn] 30 May 2014

Dimensional transition of energy cascades in stably stratified thin fluid layers

A. Sozza[1], G. Boffetta[1], P. Muratore-Ginanneschi[2], S. Musacchio[3]

[1]Department of Physics and INFN, University of Torino, via P.Giuria 1, 10125 Torino, Italy

[2]Department of Mathematics and Statistics, University of Helsinki PL 68, FIN-00014 Helsinki, Finland

[3]Université de Nice Sophia Antipolis, CNRS, LJAD, UMR 7351, 06100 Nice, France

(Received 2 June 2014)

Numerical simulations of a thin layer of turbulent flow in stably stratified conditions within the Boussinesq approximation have been performed. The statistics of energy transfer among scales have been investigated for different values of control parameters: thickness of the layer and density stratification. It is shown that in a thin layer with a quasi-two-dimensional phenomenology, stratification provides a new channel for the energy transfer towards small scales and reduces the inverse cascade. The role of vortex stretching and enstrophy flux in the transfer of kinetic energy into potential energy at small scales is discussed.

1. Introduction

In many instances of geophysical flows, the fluid motion is confined by material boundaries or other physical mechanisms in thin layers with a small aspect ratio. The thickness of such layers can be much smaller than the typical horizontal scales of motion, while being at the same time much larger than the dissipative viscous scales.

The turbulent dynamics of flows confined in quasi two-dimensional geometries exhibits a rich and interesting phenomenology. Numerical simulations (Smith et al. 1996; Celani et al. 2010) and experiments (Shats et al. 2010; Xia et al. 2011) have shown that a mixture of two-dimensional (2D) and three-dimensional (3D) dynamics can emerge in such situation. In particular, when the thickness of the fluid layer is smaller than the length scale of the forcing the turbulent cascade of kinetic energy injected by external forces splits in two parts. A fraction of the energy is transferred toward small, viscous scales as in 3D turbulence, while the remnant energy undergoes an inverse cascade toward large scales as in 2D turbulence. The key parameter which determines the energy flux of the two cascades is the ratio $S = L_z/L_f$ between the confining scale L_z and the length scale of the forcing L_f (Smith et al. 1996; Celani et al. 2010).

Beside the confinement, other physical factors can affect the effective dimensionality of geophysical flows. One important ingredient is rotation, which typically favors a two-dimensionalization of the flow (Smith & Waleffe 1999; Pouquet et al. 2013; Deusebio et al. 2014). The presence of a stable stratification of density also affects the dimensionality of geophysical flows (for a review see, e.g. Riley & Lelong (2000)). A typical feature of strongly stratified turbulent flows, which has been observed both in numerical simulations and experiments (Billant & Chomaz (2000, 2001); Smith & Waleffe (2002); Waite & Bartello (2004); Godoy-Diana et al. (2004); Praud et al. (2005); Brethouwer et al. (2007) among others), is the formation of quasi-horizontal layered structure, often called "pancakes". It has been argued by Billant & Chomaz (2000) that their formation could be connected to instabilities of columnar vortices.

The presence of these structures is accompanied by a breaking of the isotropy of the flow. In particular the vertical velocities are strongly suppressed and the horizontal flows become predominant. At the same time the strong shear between the layered structures originates intense vertical gradients of horizontal velocities. Scaling analysis by Billant & Chomaz (2001) and Lindborg (2006) predicts that the typical thickness of the layered structures L_v is proportional to the magnitude of horizontal velocity U and to the inverse of the Brunt-Väisäla frequency N. The aspect ratio between the vertical scale L_v and horizontal scale L_h of the flow is therefore proportional to the horizontal Froude number $L_v/L_h \sim F_h = U/NL_h$.

The role played by these structures on the transfer of energy in stratified turbulence has been extensively investigated because of its relevance for the dynamics of the atmosphere. Early studies by Lilly (1983) proposed the hypothesis that two-dimensional turbulence could develop within the horizontal layers, leading to the formation of an inverse energy cascade which could transfer kinetic energy toward large-scale structures. On the other hand, predictions based on eddy damped quasi-normal Markovian (EDQNM) closure by Godeferd & Cambon (1994) have argued that the formation of layered structures should block the development of an inverse energy cascade because of the strong dissipation due to the turbulent shear between layers.

Although early simulations of stratified flows by Herring & Métais (1989) reported the presence of a weak inverse cascade, most numerical simulations (Waite & Bartello (2004, 2006); Lindborg (2006); Brethouwer et al. (2007); Marino et al. (2013)) have found a direct cascade of kinetic energy. An energy transfer from small to large scale has been observed in numerical simulations by Smith & Waleffe (2002); Laval et al. (2003); Waite & Bartello (2004, 2006); Lindborg (2006) for Froude number smaller than a $O(1)$ critical value, but this phenomenon is not associated to an inverse energy cascade of vortical energy as in 2D turbulence. Conversely, kinetic energy piles up in vertically sheared horizontal flows (VSHF), i.e., shear modes with $k_h = 0, k_z \neq 0$. It has been argued that this process is the result of inertial-gravity waves interactions, but its mechanisms are still poorly understood. The situation is even more complex when the stratified flow is subject to rotation. In stably stratified rotating flows, an inverse cascade has been observed (Métais et al. 1996; Smith & Waleffe 2002; Waite & Bartello 2006; Marino et al. 2013). In particular, when rotation and stratification have comparable strength (i.e. rotation rate and Brunt-Vaisala frequency are similar), the energy transfer toward large scales is found to be larger than in the purely rotating case (Marino et al. 2013).

The picture which emerge from the results of previous studies is that in the limit of strong stratification, and in absence of rotation, the turbulent flow is characterized by a cascade toward small scales both of kinetic energy and potential energy (see, e.g., Lindborg (2006); Brethouwer et al. (2007)). These observations pose an intriguing question. Given the fact that in absence of stratification the turbulent dynamics of thin fluid layers shows the development of an inverse cascade, which on the contrary is absent in presence of a strong stratification, it is natural to investigate the physical mechanism which bridges these two extremes cases.

In this work we consider the consequences of stable stratification on a thin layer of turbulent flow and the effect on the direction of the energy cascade. By means of a set of high-resolution numerical simulations, we investigate the mechanisms of transfer of kinetic and potential energy in a stably stratified turbulent flow forced at intermediate scales and confined in fluid layers with variable aspect ratio. We show that the turbulent cascade of potential energy acquired by the fluid, acts as a new channel for dissipation which reduces the large-scale flux of kinetic energy and eventually prevents the development of the inverse cascade.

The remaining of the paper is organized as follows: Section 2 presents the governing equation and described the numerical simulations. In Section 3 we report and discuss the results obtained. Section 4 is devoted to conclusions.

2. Governing equations and numerical simulations

The equation of motion for an incompressible flow, stably stratified in the vertical direction by a mean density gradient γ, in the gravitational field $\mathbf{g} = (0, 0, -g)$ within the Boussinesq approximation are

$$\frac{\partial \mathbf{u}}{\partial t} + \mathbf{u} \cdot \boldsymbol{\nabla} \mathbf{u} = -\frac{1}{\rho_0} \boldsymbol{\nabla} p + \nu \nabla^2 \mathbf{u} - N \phi \mathbf{e}_3 + \mathbf{f} \tag{2.1}$$

$$\frac{\partial \phi}{\partial t} + \mathbf{u} \cdot \boldsymbol{\nabla} \phi = \kappa \nabla^2 \phi + N \mathbf{e}_3 \cdot \mathbf{u} \tag{2.2}$$

supplemented by the condition of incompressibility $\boldsymbol{\nabla} \cdot \mathbf{u} = 0$. Here, $\mathbf{u} = (u_1, u_2, u_3)$ is the velocity field, ϕ, which has the dimension of a velocity, is proportional to the deviation of the density field ρ from the linear vertical (z direction) profile $\rho = \rho_0 + \gamma(\phi/N - z)$, γ is the mean density gradient which, together with the acceleration of gravity g, defines the Brunt-Vaisala frequency N as $N^2 = \gamma g/\rho_0$. The parameters ν and κ are the molecular viscosity and diffusivity respectively. The flow is sustained by the external force $\mathbf{f}(\mathbf{x}, t)$, which is active on a characteristic correlation scale L_f and provides an energy input rate ε_f.

In the absence of forcing and dissipations, equations (2.1-2.2) conserve the total energy density, given by the sum of kinetic and potential contributions:

$$E = E_k + E_p = \frac{1}{2} \langle |\mathbf{u}|^2 \rangle + \frac{1}{2} \langle \phi^2 \rangle \tag{2.3}$$

where $\langle ... \rangle = \frac{1}{V} \int d^3x ...$ represents the average over the whole volume V of the fluid.

The energy balance (see Appendix A for its derivation) reads:

$$\frac{dE_K}{dt} = \varepsilon_f - \varepsilon_\nu - \varepsilon_x \ , \qquad \frac{dE_P}{dt} = \varepsilon_x - \varepsilon_\kappa \tag{2.4}$$

where we have introduced the viscous dissipation rate of kinetic energy $\varepsilon_\nu = \nu \langle \partial_i u_j \partial_i u_j \rangle$ (summation over repeated indices is assumed), the diffusive dissipation rate of potential energy $\varepsilon_\kappa = \kappa \langle \partial_i \phi \partial_i \phi \rangle$ and the exchange rate between kinetic and potential energy $\varepsilon_x = N \langle u_3 \phi \rangle$. The sign of the exchange rate ε_x is not defined a priori, but the analysis of the Kármán-Howart-Monin equations (discussed in Appendix A) shows that it is positive on average. This indicates that it causes an effective dissipation of kinetic energy and a production of potential energy, which is indeed observed in our simulations.

In the limit of vanishing stratification, $N \to 0$ the field ϕ decouples from the velocity field in (2.1) which therefore recovers the usual Navier-Stokes equation, while (2.2) becomes the equation for the evolution of a passive scalar field (which therefore does not affect the velocity field). Because in this limit (2.2) is not forced, the scalar field eventually vanishes and the energy (2.3) is dominated by the kinetic component only, which becomes an inviscid invariant.

In this limit $N = 0$, the transition from 2D to 3D turbulent phenomenology is determined by the aspect ratio $S = L_z/L_f$ between the vertical scale and the characteristic forcing scale L_f (Smith et al. 1996; Celani et al. 2010). As $S \to 0$ one recovers the 2D scenario in which the energy flux is towards the large scales $\ell \gg L_f$ and kinetic energy grows linearly at a rate $\varepsilon_\alpha = dE_K/dt$. In the limit of very small viscosity the standard 2D

phenomenology (Boffetta & Ecke 2012) predicts that $\varepsilon_\alpha = \varepsilon_f$, i.e. all the injected energy is transferred to large scale. Numerical simulations at increasing values of S have shown (Celani et al. 2010) a progressive transition toward the 3D phenomenology of direct cascade. When the vertical scale L_z becomes larger than the viscous scale, an intermediate regime with both a direct and an inverse cascade of kinetic energy appears. In this "split cascade" regime, intermediate between 2D and 3D turbulence, a fraction $\varepsilon_\alpha < \varepsilon_f$ of energy input is transferred toward large scales while the remaining energy is transferred toward small scales where it is dissipated by viscosity at a rate ε_ν. The conservation of kinetic energy gives a constraint for the sum of the fluxes of the inverse and direct energy cascade $\varepsilon_\alpha + \varepsilon_\nu = \varepsilon_f$. By increasing the aspect ratio S the ratio $\varepsilon_\nu/\varepsilon_\alpha$ increases and eventually a complete 3D phenomenology is recovered in which the system attains a stationary state with $\varepsilon_\alpha = 0$. The value of S at which the flux of the inverse cascade vanishes is not universal and may depend on the detail of the forcing. In the numerical setup adopted by Celani et al. (2010) this is observed for $S \approx 1/2$.

The main goal of our work is to investigate how the above scenario is affected by the presence of a stable stratification of density in the fluid layer. In particular we will study how the various quantities which appears in the energy balance depends both on the aspect ratio S and the Froude number Fr, and we will determine which part of the parameter space (S, Fr) allows for the development of an inverse energy cascade.

2.1. *Numerical simulations*

We performed direct numerical simulations of equations (2.1-2.2) by means of a parallel, fully dealiased, pseudo-spectral code. The flow is confined in a triply-periodic domain, with horizontal sizes $L_x = L_y = 2\pi$ and vertical size $L_z \ll L_x, L_y$. The domain is discretized on a regular grid with resolution $N_x = N_y = 512$ and $N_z = N_x(L_z/L_x)$.

In the setup of our numerical simulations, the forcing $\mathbf{f}(\mathbf{x}, t)$ which sustains the turbulent flow is a Gaussian, white-in-time stochastic noise, active only on the horizontal components of velocity (u_1, u_2) and depending on the horizontal components (x, y) only. This choice is consistent with the two-dimensional limit for $L_z \to 0$ and gives a forcing (and energy input) which is independent on the parameter L_z. The forcing is localized in the Fourier space in a narrow band of wave numbers $|\mathbf{k}| \simeq k_f = 8$ and injects energy into the system at a fixed rate ε_f. We adopt a hyperviscous damping scheme $\nu_p \nabla^{2p}$ of order $p = 8$ both for the viscosity and the diffusivity, with $\nu_p/\kappa_p = 1$.

The non-dimensional parameter which quantify the confinement is given by the ratio

$$S = \frac{L_z}{L_f} \tag{2.5}$$

between the vertical scale and the characteristic forcing scale $L_f = 2\pi/k_f$.

The intensity of the stratification is expressed in term of the Froude number, a second dimensionless number here defined as in Smith & Waleffe (2002):

$$Fr = \frac{\varepsilon_f^{1/3} k_f^{2/3}}{N} \tag{2.6}$$

It is worth to remind that this definition of the Froude number is aimed to non-dimensionalize the parameters which are fixed a priori in the simulations, and it is not based on observables which are measured a posteriori. The region of parameter space (S, Fr) explored in our simulations is shown in Table 1.

$Fr\backslash S$	0.5	0.438	0.375	0.344	0.313	0.282	0.25	0.219	0.188	0.172	0.125
∞	0.035	0.054	0.099		0.160		0.282		0.384		0.540
0.75		0.032	0.060		0.186		0.271		0.341		0.526
0.5		0.025	0.024		0.138		0.251		0.329		0.527
0.4			0.038		0.117		0.234		0.312		0.459
0.3				0.0	0.047	0.089	0.132	0.246	0.274		0.478
0.25					0.0	0.044	0.112	0.208	0.214		0.450
0.2							0.0	0.098	0.150	0.275	0.415
0.15									0.002	0.123	

TABLE 1. Parameter space of the simulations. Each number corresponds to a simulation and represents the fraction of energy transferred to large scales, $\varepsilon_\alpha/\varepsilon_f$, as a function of $Fr = (\varepsilon_f^{1/3} k_f^{2/3})/N$ and $S = L_z/L_f$.

3. Results

For each couple of parameters (Fr, S) we performed a numerical simulation starting from initial conditions $\mathbf{u}(\mathbf{x}, t = 0) = 0$ and $\phi(\mathbf{x}, t = 0) = 0$, that is with the fluid at rest and without density fluctuations. In the first stage ($t \leqslant 10\tau_f$) the flow is not yet turbulent: small scale energy dissipation is zero and kinetic energy grows at the the input rate ε_f. After this transient stage, turbulence develops and the potential energy E_P attains statistically steady values which increases as Fr is reduced (see Figure 1).

The temporal evolution of the kinetic energy $E_K(t)$ is also shown in Figure 1 for different values of Fr. In the turbulent stage, and in the absence of stratification, the energy grows linearly in time, with a rate $dE_K/dt = \varepsilon_\alpha < \varepsilon_f$ which is equal to the flux of the inverse energy cascade. By increasing the stratification this growth rate reduces, and eventually vanishes (for $Fr \simeq 0.2$ in this particular case). It is worth to notice that the kinetic energy associated to the vertical motions $\langle u_3^2 \rangle$ becomes statistically constant for any Fr, therefore the observed growth of kinetic energy is due solely to horizontal flows.

In Table 1 we report for each simulation the values of the energy growth rates ε_α, measured from the growth of $E_K(t)$, normalized with the energy input ε_f. We remind that this ratio is equal to the fraction of energy which is transferred to large scales producing the inverse energy cascade.

For fixed values of Fr the ratio $\varepsilon_\alpha/\varepsilon_f$ is a decreasing function of the aspect ratio S (see Figure 2), and vanishes for a critical aspect ratio $S_c(Fr)$ which becomes smaller as the stratification increases. The behavior of S_c (determined by linear interpolation of the lines displayed in Fig. 2) as a function of Fr is shown in Figure 3. In the limit of vanishing stratification $Fr \to \infty$ the critical aspect ratio is bounded by the value $S_c \simeq 1/2$ which is observed in absence of stratification (Celani et al. 2010). For sufficiently strong stratification we find that the S_c becomes smaller and follows, for small Fr, approximately the scaling $S_c \simeq Fr$.

The scaling of the critical aspect ratio $S_c \simeq Fr$ provides a crucial indication to understand the mechanism which causes the suppression of the inverse energy cascade induced by stratification. In analogy with the aspect ratio S, which expresses the ratio between the confining scale L_z and the forcing scale L_f, also the Froude number can be rewritten as the ratio between the characteristic vertical scale of the layered structures which

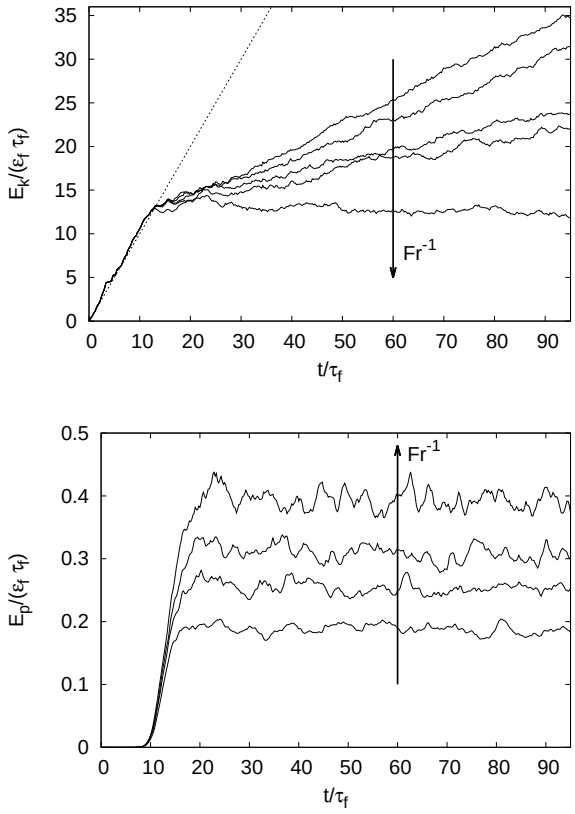

FIGURE 1. Temporal evolution of kinetic energy $E_K(t)$ (upper) and potential energy $E_P(t)$ (lower) at $S = 0.25$. Froude numbers are $Fr = 0.2$, 0.25, 0.3, 0.4 and $Fr = \infty$.

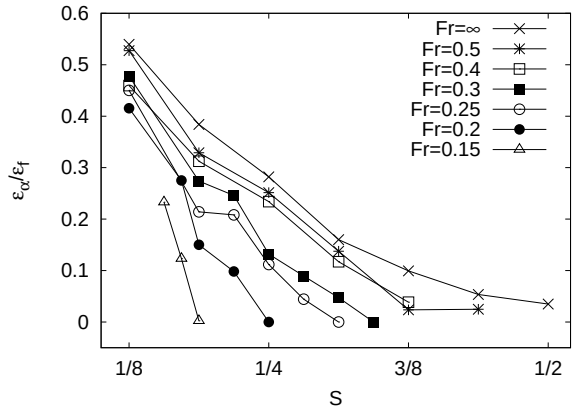

FIGURE 2. Growth rates of kinetic energy ε_α (measured from the growth rate of $E_K(t)$) normalized with the energy input ε_f, as a function of the aspect ratio $S = L_z/L_f$ for different Fr.

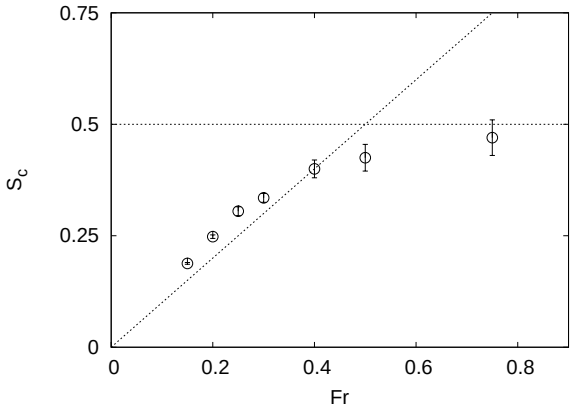

FIGURE 3. Critical aspect ratio S_c, estimated from the data in Fig. 2, as a function of Fr.

characterize the stratified flows $L_v = \varepsilon_f^{1/3} L_f^{1/3}/N$ and the forcing scale L_f:

$$\frac{L_v}{L_f} = \frac{\varepsilon_f^{1/3} L_f^{-2/3}}{N} \simeq Fr \tag{3.1}$$

The condition to achieve a complete suppression of the inverse cascade $S \simeq Fr$ is therefore equivalent to the condition $L_z \simeq L_v$. This suggest a relation between the formation of layered structures and the suppression of the inverse cascade. In a layer with a given height L_z the inverse cascade disappears when the stratification is sufficiently strong such that the typical thickness of the pancake structures becomes small enough to fit in the fluid layer. From a dynamical point of view, the suppression of the inverse cascade means that the kinetic energy is not transported to large scale and this requires that a different term in the energy transfer becomes relevant.

Let us therefore consider the fraction of energy which is transported toward small scales. In Figure 4 we show the dissipation rate of kinetic energy ε_ν and potential energy ε_κ due respectively to the viscosity and molecular diffusivity. Both quantities are normalized with the total dissipation $\varepsilon_T = \varepsilon_\nu + \varepsilon_\kappa$. In the limit of vanishing stratification $Fr \to \infty$ one has trivially $\varepsilon_\nu/\varepsilon_T \to 1$ and $\varepsilon_\kappa/\varepsilon_T \to 0$. At increasing the stratification the fraction of energy dissipated by viscosity reduces, while the energy dissipation due to diffusivity grows. Our findings suggest that in the limit of strong stratification $Fr \to 0$ the two dissipations may become of the same order $\varepsilon_\nu \simeq \varepsilon_\kappa$. It is interesting to note that the ratios $\varepsilon_\nu/\varepsilon_T$ and $\varepsilon_\kappa/\varepsilon_T$ do not show a strong dependence on the aspect ratio S.

We remark that, because from energy balance we have $\varepsilon_f = \varepsilon_\alpha + \varepsilon_T$, the decrease of ε_α with Fr^{-1} shown in Fig. 1 corresponds to an increase of total dissipation ε_T with stratification.

The exchange rate from kinetic to potential energy $\varepsilon_x = N\langle u_3\phi\rangle$ is shown in Figure 5. The sign of ε_x is always positive, indicating that there is an irreversible conversion of kinetic energy into potential energy which is dissipated by the turbulent diffusivity. We find that the exchange rate decays approximatively as $\varepsilon_x \sim Fr^{-1}$, and grows as the aspect ratio S is increased.

In Figure 6 we show the probability density function (PDF) of the local exchange rate $\chi \equiv N u_3\phi$ (with $\varepsilon_x = \langle\chi\rangle$) for different values of Fr and S. The PDFs are non-Gaussian and they are characterized by broad negative and positive tails. This implies that the mean positive value of χ, which indicates the mean preferential transfer of energy from

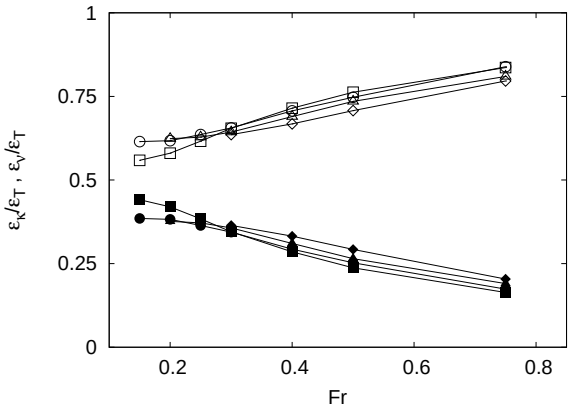

FIGURE 4. Kinetic ε_ν (open symbols) and potential ε_κ (filled symbols) energy dissipation rates normalized by the total dissipation $\varepsilon_T = \varepsilon_\nu + \varepsilon_\kappa$ as a function of Fr for different $S = 0.125$ (squares), $S = 0.188$ (circles), $S = 0.25$ (triangles) and $S = 0.313$ (diamonds).

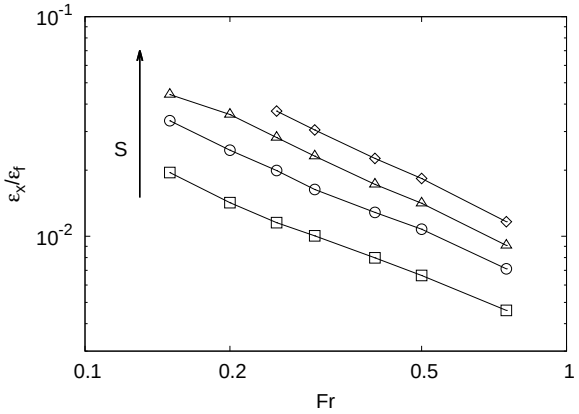

FIGURE 5. Exchange rates between kinetic and potential energy ε_x normalized with the energy input ε_f, as a function of Fr for different $S = 0.125$ (squares), $S = 0.188$ (circles), $S = 0.25$ (triangles) and $S = 0.313$ (diamonds).

kinetic to potential, is the results of strong cancellations between local events of intense energy transfer in both directions. We find that the asymmetry of the PDFs reduces as Fr decreases, and that the right tail grows as the aspect ratio S is reduced. The intermittent behavior of the energy transfer revealed by the broad tails of the PDFs of the local exchange rate $\chi \equiv Nu_3\phi$ is in agreement with recent findings by Rorai et al. (2014) which have shown that also the PDFs of ϕ and u_3 have non-Gaussian behavior.

3.1. *Spectral fluxes*

More detailed information on the mechanism of energy transfer are provided by the inspection of the fluxes of kinetic and potential energy

$$\Pi_K(k) = \int_{|\boldsymbol{q}|\leqslant k} d\boldsymbol{q}(\boldsymbol{u}\cdot\nabla\boldsymbol{u})(\boldsymbol{q})\boldsymbol{u}^*(\boldsymbol{q}) \tag{3.2}$$

$$\Pi_P(k) = \int_{|\boldsymbol{q}|\leqslant k} d\boldsymbol{q}(\boldsymbol{u}\cdot\nabla\boldsymbol{\phi})(\boldsymbol{q})\boldsymbol{\phi}^*(\boldsymbol{q}) \tag{3.3}$$

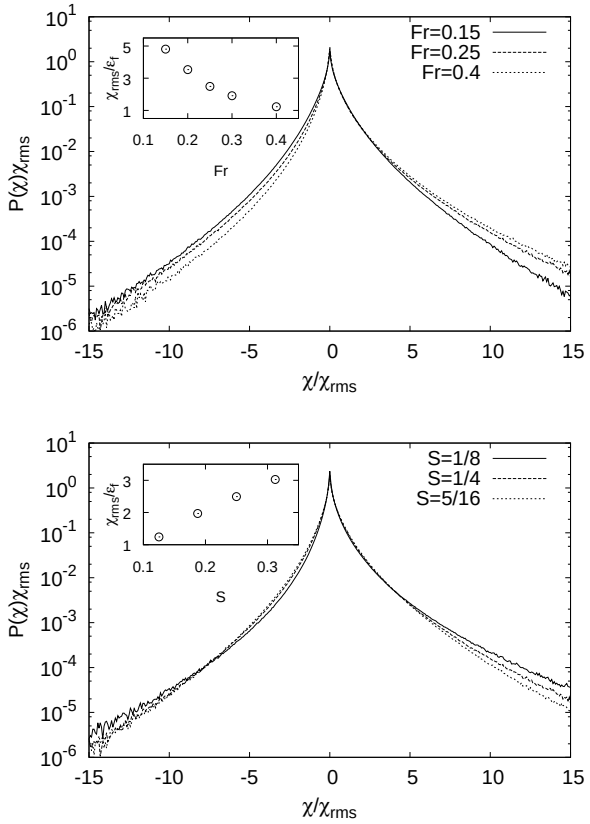

FIGURE 6. Probability density functions of the local exchange term χ (rescaled with the rms value) for different values of Fr at $S = 0.25$ (upper panel) and different S at $Fr = 0.25$ (lower panel). In the insets the dependence of the rms value χ_{rms} on Fr and S is shown.

In absence of stratification the spectral flux of kinetic energy $\Pi_K(k)$ displays two plateau (see Figure 7). At small wavenumbers $k < k_f$ the energy flux is negative, signaling the presence of an inverse energy cascade. At large wavenumbers $k > k_f$ the positive plateau of the flux indicates the direct energy cascade towards small scales.

The presence of a stable stratification of density affects the double cascade of kinetic energy in both ranges of wavenumbers. At small wavenumbers the flux of the inverse cascade is reduced with the stratification, as Fr decreases. Simultaneously, in the range of wavenumbers $k_f < k < k_z$ the flux of kinetic energy toward small scales is enhanced.

At large wavenumbers $k > k_z$ (larger than the wavenumber associated to the thickness of the fluid layer $k_z = 2\pi/L_z = k_f/S$) we observe the development of a cascade of potential energy, whose flux grows as Fr decreases. The direct cascade of potential energy develops at the expenses of the kinetic energy, whose flux shows a significative reduction at large wavenumbers $k > k_z$. Remarkably, at very large wavenumbers $k \gg k_z$, the fluxes of kinetic energy are always smaller than in the non-stratified case, although they display a weak growth at increasing stratification. This indicates that the main effect of the vertical shears associated to the layered structures in stratified flows is to promote the conversion of kinetic energy into potential energy, rather than to cause an enhancement of the viscous dissipation.

The conversion of kinetic energy into potential energy is a process which requires to

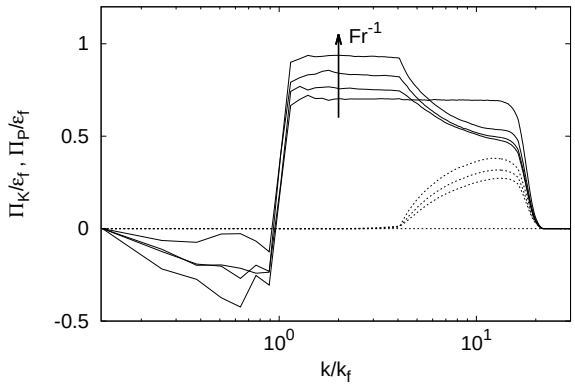

FIGURE 7. Spectral fluxes of kinetic energy (solid lines) and potential energy (dotted lines) for different values of Froude number ($Fr = \infty$, $Fr = 0.3$, $Fr = 0.25$, $Fr = 0.2$ from bottom to top) and fixed aspect ratio ($S = 1/4$)

move a parcel of fluid in the vertical direction. Its efficiency is therefore strongly affected by the thickness of the fluid layer. The space required in the vertical direction to achieve the maximum conversion is of the order of the thickness of the pancake structures L_v. If the depth of the fluid layer L_z is thinner than L_v it is possible to achieve only a partial conversion, allowing for the survival of a remnant inverse energy cascade toward large scales. The inverse cascade is completely suppressed when the layer is sufficiently thick or the stratification is sufficiently strong, such that $L_z > L_v$, allowing for the maximum conversion of kinetic energy into potential energy. This picture is consistent with the scaling $S_c \simeq Fr$ observed in Figure 3.

In absence of stratification, a crucial role in determining the ratio between the fluxes of kinetic energy of the direct and inverse cascade is played by the phenomenon of vortex stretching. In three-dimensional flows, the vortex stretching is responsible for the production of enstrophy which is related to the rate of viscous dissipation of energy and therefore to the flux of energy in the direct cascade. Conversely, in ideal two-dimensional flows, the term responsible for the vortex stretching vanishes, and enstrophy becomes an inviscid invariant. The joint conservation of enstrophy and energy causes the reversal of the energy cascade which is transferred toward large scales.

In the case of a fluid layer with a finite thickness L_z smaller than the forcing scale L_f we observe the phenomenon shown in Figure 8. The spectral flux of enstrophy Π_Z and the spectral production of enstrophy Σ_Z are defined as

$$\Pi_Z = \int_{|\boldsymbol{q}|\leqslant k} d\boldsymbol{q}(\boldsymbol{v}\cdot\nabla\boldsymbol{\omega})(\boldsymbol{q})\boldsymbol{\omega}^*(\boldsymbol{q}) \tag{3.4}$$

$$\Sigma_Z = \int_{|\boldsymbol{q}|\leqslant k} d\boldsymbol{q}(\boldsymbol{\omega}\cdot\nabla\boldsymbol{v})(\boldsymbol{q})\boldsymbol{\omega}^*(\boldsymbol{q}) \tag{3.5}$$

In the non-stratified case ($Fr = \infty$) the enstrophy flux is constant in the range $k_f < k < k_z$, indicating the presence of a direct cascade of enstrophy, consistent with a quasi-two-dimensional phenomenology. The enstrophy production is activated only at $k > k_z$ where therefore the enstrophy flux is not conserved. In the stratified case ($Fr = 0.2$ in Figure 8) the enstrophy flux remains unchanged in the range $k_f < k < k_z = k_f/S$. At higher wavenumber we do not observe a relevant increase of the production of enstrophy, which remains similar to the non-stratified case. On the contrary, the flux of enstrophy

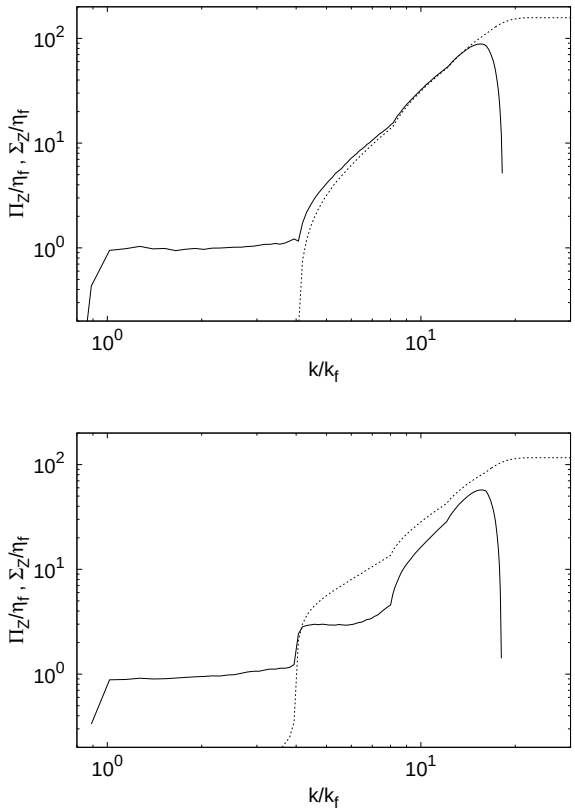

FIGURE 8. Spectral flux of enstrophy Π_ω (solid line) and vortex-stretching Σ_ω (dashed line) for simulations at $S = 0.25$ and $Fr = \infty$ (upper panel) and $Fr = 0.2$ (lower panel). All quantities are normalized by the enstrophy input by forcing.

is reduced, signaling that a fraction of the enstrophy generated by the vortex stretching is spent in the process of conversion of kinetic energy into potential energy.

4. Conclusions

We have investigated the direction of the energy flux in a set of numerical simulations of a thin layer of stratified fluid for different values of stratification (Froude number Fr) and thickness (aspect ratio S). We have shown that, in general, stratification reduces the intensity of the inverse cascade and, consequently, the critical value of stratification S_c at which the inverse flux vanishes.

For small values of Fr, this critical number is found to grow approximatively as $S_c \simeq Fr$. This fact supports the picture by which the inverse cascade vanishes when the thickness of the pancake structures in the flow is sufficiently small to fit into the fluid layer. For larger values of Fr, the critical aspect ratio is found to recover the unstratified limit.

A spectral analysis of the kinetic and potential energy fluxes shows that the suppression of the inverse cascade of kinetic energy is accompanied by the generation of a direct cascade of potential energy which becomes an alternative channel for the transfer and dissipation of injected energy.

Our findings open new pespectives for both experimental and theoretical research in turbulence.

Stable stratification of density has been often used in experimental setup of electromagnetically-forced thin fluid layers with the purpose of suppressing vertical motions and enhancing the two-dimensionality of the flow. It would be interesting to observe experimentally the suppression of the inverse cascade at increasing the stratification, and to compare the results with our numerical findings.

From a theoretical point of view it would be extremely useful to have a predictive phenomenological model which allows to determine the fraction of energy which is drained by the direct cascade of potential energy, and therefore to have a quantitative prediction for the suppression of the inverse energy cascade as function of both the aspect ratio and the stratification.

Authors are grateful to Filippo De Lillo and Enrico Deusebio for fruitful discussions. Numerical simulations were performed on the INFN Turbofarm cluster in Turin, Italy.

Appendix A. Kármán-Howart-Monin equation for stratified turbulence

In this Appendix we derive a set of generalized Kármán-Howart-Monin (KHM) equation for stably stratified turbulence.

We define the velocity and scalar two-point correlation functions as:

$$C_2^{(u)}(\mathbf{x},t) \equiv \langle \mathbf{u}(\mathbf{x},t)\cdot\mathbf{u}(\mathbf{0},t)\rangle \tag{A 1}$$

$$C_2^{(\phi)}(\mathbf{x},t) \equiv \langle \phi(\mathbf{x},t)\phi(\mathbf{0},t)\rangle \tag{A 2}$$

and the correlation among the two fields, representing the exchange of energy between kinetic and potential

$$C_{1,1}^{(u_3,\phi)}(\mathbf{x},t) \equiv \langle u_3(\mathbf{x},t)\phi(\mathbf{0},t)\rangle\,. \tag{A 3}$$

Dissipation of kinetic and potential energy are defined as ($\alpha,\beta = 1,2,3$ and we sum over repeated index)

$$D^{(u)}(\mathbf{x},t) \equiv 2\nu\langle(\partial_\alpha u_\beta)(\mathbf{x},t)(\partial_\alpha u_\beta)(\mathbf{0},t)\rangle \tag{A 4}$$

$$D^{(\phi)}(\mathbf{x},t) \equiv 2\kappa\langle(\partial_\alpha \phi)(\mathbf{x},t)(\partial_\alpha \phi)(\mathbf{0},t)\rangle \tag{A 5}$$

and cross dissipation as

$$D^{(u,\phi)}(\mathbf{x},t) \equiv 2\nu\langle(\partial_\alpha \phi)(\mathbf{x},t)(\partial_\alpha u_3)(\mathbf{0},t)\rangle + 2\kappa\langle(\partial_\alpha u_3)(\mathbf{x},t)(\partial_\alpha \phi)(\mathbf{0},t)\rangle \tag{A 6}$$

The correlation of the two-dimensional, two-component forcing $\mathbf{f}(\mathbf{x},t)$ is given by

$$\langle f_i(\mathbf{x},t) f_j(\mathbf{0},0)\rangle = \delta_{ij}\delta(t)F(r_h/L_f) \tag{A 7}$$

where $i,j = 1,2$ and $r_h^2 = x_1^2 + x_2^2$ is the separation on the horizontal plane and $F(x)$ is the spatial correlation.

The Kármán-Howart-Monin equations will involve also third-order structure functions. In particular we define

$$\mathbf{S}_3^{(u)}(\mathbf{x},t) \equiv \langle[\mathbf{u}(\mathbf{x},t)-\mathbf{u}(\mathbf{0},t)]|\mathbf{u}(\mathbf{x},t)-\mathbf{u}(\mathbf{0},t)|^2\rangle \tag{A 8}$$

$$\mathbf{S}_{1,2}^{(u,\phi)}(\mathbf{x},t) \equiv \langle[\mathbf{u}(\mathbf{x},t)-\mathbf{u}(\mathbf{0},t)][\phi(\mathbf{x},t)-\phi(\mathbf{0},t)]^2\rangle \tag{A 9}$$

$$\mathbf{S}_{2,1}^{(u_3,\phi)}(\mathbf{x},t) \equiv \langle [\mathbf{u}(\mathbf{x},t)-\mathbf{u}(\mathbf{0},t)][u_3(\mathbf{x},t)+\phi(\mathbf{x},t)-u_3(\mathbf{0},t)-\phi(\mathbf{0},t)]^2\rangle \qquad (A\,10)$$

Starting from (2.1-2.2), by exploiting homogeneity and incompressibility, we derive a set of generalized KHM equations, the first for kinetic energy

$$\frac{\partial C_2^{(u)}(\mathbf{x},t)}{\partial t} + D^{(u)}(\mathbf{x},t) + NC_{1,1}^{(u_3,\phi)}(\mathbf{x},t) = F(\mathbf{x}) + \frac{1}{2}\boldsymbol{\nabla}\cdot\mathbf{S}_3^{(u)}(\mathbf{x},t) \qquad (A\,11)$$

and the second for potential energy

$$\frac{\partial C_2^{(\phi)}(\mathbf{x},t)}{\partial t} + D^{(\phi)}(\mathbf{x},t) - NC_{1,1}^{(u_3,\phi)}(\mathbf{x},t) = \frac{1}{2}\boldsymbol{\nabla}\cdot\mathbf{S}_{1,2}^{(u,\phi)}(\mathbf{x},t) \qquad (A\,12)$$

At variance with the usual Navier-Stokes equation (Frisch 1995), (A 11) involves the additional term $C_{1,1}^{(u_3,\phi)}$ which represents the transfer of energy from kinetic to potential term. The equivalent of the KHM equation for the exchange energy reads

$$\frac{\partial C_{1,1}^{(u_3,\phi)}(\mathbf{x},t)}{\partial t} + D^{(u_3,\phi)}(\mathbf{x},t) - 2NC_2^{(u_3)}(\mathbf{x},t) + 2NC_2^{(\phi)}(\mathbf{x},t) = \frac{1}{2}\boldsymbol{\nabla}\cdot\mathbf{S}_{2,1}^{(u,\phi)}(\mathbf{x},t) \quad (A\,13)$$

Adding up (A 11) and (A 12), this energy exchange terms cancels and we get the KHM relation for the total energy

$$\frac{\partial}{\partial t}\left(C_2^{(u)}(\mathbf{x},t)+C_2^{(\phi)}(\mathbf{x},t\right)+\left(D^{(u)}(\mathbf{x},t)+D^{(\phi)}(\mathbf{x},t)\right) = F(\mathbf{x})+\frac{1}{2}\boldsymbol{\nabla}\cdot\left(\mathbf{S}_3^{(u)}(\mathbf{x},t)+\mathbf{S}_{1,2}^{(u,\phi)}(\mathbf{x},t)\right) \qquad (A\,14)$$

For $\mathbf{x}\to 0$, at finite ν and κ, (A 14) gives the energy balance equation

$$\frac{d}{dt}(E_k+E_p)+\varepsilon_\nu+\varepsilon_\kappa=\varepsilon_f \qquad (A\,15)$$

where $\varepsilon_f = F(0)/2$ is the energy input and ε_ν and ε_κ are the viscous and diffusive energy dissipations respectively. In the absence of stratification, usual Navier-Stokes equations in 3D reach a steady state in which $\varepsilon_\nu=\varepsilon_f$ and $dE/dt=0$. This is not the case in 2D, where the inverse cascade transfers kinetic energy to large scales where viscous dissipation is not effective (in the limit of large Reynolds numbers). Previous investigations and our numerical simulations show that also in presence of stratification total energy reaches a steady state, indicating the absence of inverse cascade. Therefore in the following we will assume stationarity.

Starting from equation (A 11) and assuming stationarity and dissipative anomaly for the kinetic energy in the limit of vanishing viscosity, one gets:

$$\lim_{\nu\to 0}\lim_{|\mathbf{x}|\to 0}\left\{D^{(u)}(\mathbf{x})+NC_{1,1}^{(u_3,\phi)}(\mathbf{x})-F(\mathbf{x})\right\}=0 \qquad (A\,16)$$

which means that the energy input is partly dissipated and partly transferred to the potential energy:

$$D^{(u)}(\mathbf{0})+NC_{1,1}^{(u_3,\phi)}(\mathbf{0})=F(\mathbf{0}) \qquad (A\,17)$$

Furthermore, taking the same limits of equation (A 11) but now in inverse order yields

$$\frac{1}{2}\lim_{|\mathbf{x}|\to 0}\lim_{\nu\to 0}\boldsymbol{\nabla}\cdot\mathbf{S}_3^{(u)}(\mathbf{x},t) = -\left\{F(\mathbf{0})-NC_{1,1}^{(u_3,\phi)}(\mathbf{0})\right\}\leqslant 0 \qquad (A\,18)$$

The negative value of the divergence is the hallmark of the direct energy cascade. The relation is thus agreement with the presence exhibited in Figure (7) of a direct energy cascade for any value of Fr.

In a similar way, assuming stationarity and dissipative anomaly for the potential energy in the limit of vanishing diffusivity in equation A 12 one gets:

$$\lim_{\kappa\to 0}\lim_{|\mathbf{x}|\to 0}\left\{D^{(\phi)}(\mathbf{x}) - NC_{1,1}^{(u_3,\phi)}(\mathbf{x})\right\} = 0 \tag{A 19}$$

and hence:

$$D^{(\phi)}(\mathbf{0})) = NC_{1,1}^{(u_3,\phi)}(\mathbf{0})) \geqslant 0 \tag{A 20}$$

This means that the cross-correlation $C_{1,1}^{(u_3,\phi)}$, being equal to the dissipation of potential energy, is positive definite. Therefore, it acts as a source term for the potential energy and as a dissipation for the kinetic energy.

REFERENCES

Billant, P., & Chomaz, J.-M. 2000 Experimental evidence for a new instability of a vertical columnar vortex pair in a strongly stratified fluid, *J. Fluid Mech.*, **418**, 167–188.

Billant, P., & Chomaz, J.-M. 2001 Self-similarity of strongly stratified inviscid flows. *Phys. Fluids*, **13**, 1645.

Boffetta, G., & Ecke, R.E. 2013 Two-dimensional Turbulence *Ann. Rev. Fluid Mech.*, **44**, 427–451.

Brethouwer, G., Billant, P., Lindborg, E., & Chomaz, J.M. 2007 Scaling analysis and simulation of strongly stratified turbulent flows. *J. Fluid Mech.*, **585**, 343–368.

Celani, A., Musacchio, S.,& Vincenzi, D. 2010 Turbulence in more than two and less than three dimensions. *Phys. Rev. Lett.*, **104**, 18.

E. Deusebio, G. Boffetta, E. Lindborg & S. Musacchio 2014 Dimensional transition in rotating turbulence. *Phys. Rev. E*, submitted.

U. Frisch 1995 Turbulence. *Cambridge University Press.*

Godeferd, F. S. & Cambon, C. 1994 Detailed investigation of energy transfer in homogeneous stratified turbulence. *Phys. Fluids* **6**, 2084–2100.

Godeferd, F. S. & Staquet, C. 2003 Statistical modelling and direct numerical simulations of decaying stably stratified turbulence. Part 2. Large-scale and small-scale anisotropy. *J. Fluid Mech.* **486**, 115–159.

Godoy-Diana, R., Chomaz, J. M. & Billant, P. 2004 Vertical length scale selection for pancake vortices in strongly stratified viscous fluids. *J. Fluid Mech.* **504**, 229–238.

Herring, J. R., & Métais, O. 1989 Numerical experiments in forced stably stratified turbulence. *J. Fluid Mech.*, **202**, 97–115.

Laval, J.-P. McWilliams, J. C & Dubruelle, B. 2003 Forced stratified Turbulence: successive transitions with Reylonds number. *Phys. Rev. E* **68**, 036308.

Lilly, D. K. 1983 Stratified turbulence and the mesoscale variability of the atmosphere. *J. Atm. Sciences*, **40**, 749–761.

Lindborg, E. 2006 The energy cascade in a strongly stratified fluid. *J. Fluid Mech.*, **550**, 2007–242.

Lindborg, E. & Brethouwer, G. 2007 Stratified Turbulence forced in rotational and divergent modes. *J. Fluid Mech.*, **586**, 83–108.

Marino, R. , Mininni, P.D. , Rosenberg, D. & Pouquet, A. 2013 Inverse cascades in rotating stratified turbulence: Fast growth of large scales. *Europhys. Lett.*, **102**, 44006.

Métais, O., Bartello, P., Garnier, E., Riley, J.J., & Lesieur, M. 1996 Inverse energy cascade in stably stratified rotating turbulence. *Dyn. Atmos. Oceans*, **23**, 193–203.

Pouquet, A., Sen, A., Rosenberg, D., Mininni, P.D., & Baerenzung, J. 2013 Inverse cascades in turbulence and the case of rotating flows. *Physica Scripta*, **T155**, 014032.

Praud, O., Fincham, A. M., Sommeria J. 2005 Decaying grid turbulence in a strongly stratified fluid. *J. Fluid Mech.*, **522**, 1–33.

Riley, J. J., & Lelong, M. P., 2000 Fluid Motions in the Presence of Strong Stable Stratification. *Ann. Rev. Fluid Mech.*, **32**, 613–657.

Rorai, C., Mininni, P.D. & Pouquet, A. 2014 Turbulence comes in burst in stably stratified flows. *Phys. Rev. E*, **89**, 043002.

Shats, M., Byrne, D., Xia, H. 2010 Turbulence Decay Rate as a Measure of Flow Dimensionality. *Phys. Rev. Lett.*, **105**, 264501.

Smith, L. M., Chasnov, J., & Waleffe, F. 1996 Crossover from Two- to Three-Dimensional Turbulence. *Phys. Rev. Lett.*, **77**, 2467.

Smith, L. M.,& Waleffe, F. 1999 titolo. *Phys. Fluids*, **11**, 1608.

Smith, L. M.,& Waleffe, F. 2002 Generation of slow large scales in forced rotating stratified turbulence. *J. Fluid Mech.*, **451**, 145–168.

Waite, M. L. 2011 Stratified turbulence at the buoyancy scale. *Phys. Fluids*, **23**, 066602.

Waite, M. L., & Bartello P. 2004 Stratified turbulence dominated by vortical motion. *J. Fluid Mech.*, **517**, 281–308.

Waite, M. L., & Bartello P. 2006 Stratified turbulence generated by internal gravity waves. *J. Fluid Mech.*, **546**, 313–339.

Xia, H., Byrne, D., Falkovich, G. & Shats, M. 2011 Upscale energy transfer in thick turbulent fluid layers. *Nat. Phys.*, **7**, 321–324.